Astron. Astrophys. 356, 735–746 (2000)

ASTRONOMY AND ASTROPHYSICS

The Green's function method for a special class of linear three-dimensional magnetohydrostatic equilibria

G.J.D. Petrie and T. Neukirch

School of Mathematical and Computational Sciences, University of St. Andrews, St. Andrews, Scotland KY16 9SS

Received 28 September 1999 / Accepted 7 February 2000

Abstract. We present the Green's function method for a special class of linear self-consistent three-dimensional solutions of the magnetohydrostatic (MHS) equations for which the current density is a combination of a linear force-free part and a part with non-forc e-free components. This allows the construction of MHS solutions of this class with arbitrary photospheric boundary conditions for B_z. These solutions can be used to extrapolate coronal magnetic fields from known longitudinal photospheric field data and provide a self-consistent description of magnetic field, plasma pressure, plasma density and plasma temperature. The method therefore allows a better comparison of models with observations of solar coronal structures. We will demonstrate how the method works by giving an illustrative example.

Key words: Sun: corona – Sun: magnetic fields – magnetic fields – methods: analytical

1. Introduction

Observations of the solar corona, especially in X-rays and EUV, show that its spatial and temporal structure is dominated by the coronal magnetic field. The determination of the magnetic field structure in the solar corona is therefore a prime task of solar physics. However, the coronal magnetic field cannot be measured directly with present techniques. Hence the coronal magnetic field has to be calculated by extrapolation from data taken at photospheric level. Any extrapolation method relies on assumptions about the electric current density in the corona. Existing extrapolation methods include potential (e.g. Schmidt 1964; Semel 1967; Schatten et al. 1969; Altschuler & Newkirk 1969), linear force-free (e.g. Chiu & Hilton 1977; Barbosa 1977; Alissandrakis 1981; Semel 1988; Gary 1989) and nonlinear force-free fields (e.g. Sakurai 1981; Wu et al. 1985; Aly 1989; McClymont & Mikic 1994; Roumeliotis 1996; Amari et al. 1997; McClymont et al. 1997; Lee et al. 1999). Details of the various methods for magnetic field reconstruction and discussion of their relative merits and limitations can be found in the review papers of e.g. Amari & Démoulin (1992), Démoulin et al. (1997), McClymont et al. (1997) and Amari et al. (1997).

Send offprint requests to: G.J.D. Petrie, (gordonp@mcs.st-and.ac.uk)

Apart from the well-known limitations of potential and linear force-free field reconstruction (Amari et al. 1997, 1999) a general problem of all reconstruction methods is that their success in representing the "true" coronal magnetic field is difficult to assess. The present paper tries to address this particular problem. We emphasise that it is not suggested here that the method presented is a better method for reconstructing the magnetic field than the linear force-free reconstruction method. In our opinion the advantage of the present method over linear force-free reconstruction is the possibility of comparing the calculated model plasma properties with observations. This is in contrast to the usual way of assessing reconstructed magnetic field lines, which is to carry out a visual comparison of a number of field lines with the observed plasma emission patterns. In a stationary model, the only possibility of allowing for spatial variations of the plasma properties (apart from stratification by gravity) is by including currents flowing perpendicular to the magnetic field. Therefore the three-dimensional stationary plasma structures imply the existence of perpendicular currents, i.e. deviations from a force-free field. Strictly speaking, the only structuring of the plasma allowed in a potential or force-free field is stratification by the gravitational force. Such a structure cannot match the observed emission patterns. Approaches towards overcoming this problem include e.g. rendering techniques (Gary 1997) and testing the consistency of physical properties of loops with the calculated field line structure (Lee et al. 1999).

However, in the solar corona the perpendicular currents necessary to explain most of the observed structures will be much smaller than the field-aligned currents determining the structure of the magnetic field. It turns out that this is also the case for the method presented here. We will see that only very small perpendicular currents are necessary to produce significant structuring of the plasma if the average plasma beta is small. In principle, one could imagine an expansion procedure in which the force-free current and the boundary conditions determine the large-scale structure of the magnetic field in the lowest order and the perpendicular currents determine the spatial structure of the plasma in the next order. A more straightforward approach is to take the perpendicular currents directly into account in the solution of the MHS equations and this is the approach we will follow in the present contribution. A non-trivial difficulty with this approach is that three-dimensional MHS equilibria have to be used

and their calculation is a problem in itself. We will use a special class of analytical self-consistent three-dimensional MHS equilibria which has been discovered by Low (1985, 1991, 1992, 1993a, b) and Bogdan & Low (1986), with some additions made by Neukirch (1995, 1997a, b). A subset of this class of equilibria has already been used to model the large-scale corona globally using spherical coordinates (e.g. Bagenal & Gibson 1991; Zhao & Hoeksema 1993, 1994; Gibson & Bagenal 1995). This subset can be derived by a simple transformation of potential or linear force-free solutions and has also recently been used for local smaller-scale modelling (Gary & Alexander 1999). All other contributions using this class of MHS solutions for the purpose of modelling local coronal structures, e.g. prominences, using Cartesian coordinates (e.g. Aulanier et al. 1998, 1999) rely on expansions of the solutions in discrete (normal) modes.

Most extrapolation methods for potential and linear force-free fields are based on the general mathematical method of Green's functions (e.g. Schmidt 1964; Semel 1967; Chiu & Hilton 1977; Allissandrakis 1981; Sakurai 1982; Semel 1988; Gary 1989). Exceptions are extrapolation methods for the global solar magnetic field using (synoptic) magnetic maps of the complete solar surface where an expansion in spherical harmonics is usually used (e.g. Schatten et al. 1969; Altschuler & Newkirk 1969; Altschuler et al. 1974, 1977). All of these methods use either the photospheric field component perpendicular to the solar surface or the line-of-sight component as input and give all magnetic field components in the complete domain as output.

The purpose of this paper is to develop the Green's function method for the special class of MHS equilibria mentioned above. We will use the results of Neukirch & Rastätter (1999) who showed that it is possible to express the magnetic field of this solution class by a single scalar function in the same way as for the linear force-free case. This result can be used to calculate the Green's function in a way completely analogous to the linear force-free case. The use of the Green's function method allows boundary conditions to be imposed which do not have to be periodic. The method enables us to calculate not only the magnetic field, but also the plasma pressure, the plasma density and the plasma temperature from the boundary data. This makes a much better comparison of the models with the observations possible.

It is, however, necessary to mention some limitations of the models. First of all, the price we pay for an analytical description of the complex plasma-magnetic field interaction is finding the equation of state of the plasma as a result rather than having it as an a priori condition. This could lead to results which are unreasonable from a physical point of view. Furthermore, the resulting magnetic fields share the deficiencies of linear force-free fields: they cannot represent different length scales as α is constant, they are not uniquely determined by the z-component of the magnetic field on the boundary and they have infinite magnetic energy if considered in an unbounded domain. Therefore we consider these models only as a first step on the way to better and more realistic models. We believe that the disadvantages just described are more than compensated for by the possibility of an analytical treatment.

The paper is organised in the following way. In Sect. 2 we summarize the necessary facts about the solution class used. In Sect. 3 we show how the representation of the magnetic field by a single scalar function (which we call the P-representation for short) simplifies the calculation of the Green's function. In Sect. 4, we show three particularly interesting special cases, starting with the linear force-free case as reference case. In Sect. 5 we show an example solution calculated by using the Green's function method and we summarize our results in Sect. 6.

2. The solution class

We are looking for three-dimensional solutions to the MHS equations

$$(\nabla \times \mathbf{B}) \times \mathbf{B} - \nabla p - \rho \nabla \psi = 0, \tag{1}$$

$$\nabla \times \mathbf{B} = \mu_0 \mathbf{j} \tag{2}$$

$$\nabla \cdot \mathbf{B} = 0 \tag{3}$$

where p = pressure, ρ = density and $\psi = gz$ = gravitational potential. Quite generally, solutions to this set of partial differential equations varying in all three spatial directions are hard to find. Therefore we follow Low (1991, 1992) and assume that Ampère's law has the form

$$\mu_0 \mathbf{J} = \nabla \times \mathbf{B} = \alpha \mathbf{B} + \nabla \times (F \nabla \psi) \tag{4}$$

where F is arbitrary, with the constraint that ∇F and $\nabla \psi$ have to be linearly independent vector fields, and α is constant (n.b. Eq. (3) immediately follows). The last term is the link between the magnetic field and the plasma (if $F = 0$ the field is force-free). Using this special form for the current density the force-balance equation Eq. (1) has only two components in the ∇F and $\nabla \psi$ directions. Let $F = K(\psi)\mathbf{B} \cdot \nabla \psi$, where $K(\psi)$ is a free function, so that these two components can be integrated:

$$p = p_0(\psi) - \frac{1}{2\mu_0 K(\psi)} F^2 \tag{5}$$

$$\rho = -\left(\frac{\partial p}{\partial \psi}\right)_F + \frac{1}{\mu_0} \mathbf{B} \cdot \nabla F. \tag{6}$$

In Cartesian coordinates we have $\psi = gz$ and $F = \frac{1}{g}\xi(z) B_z$ where $\xi(z)$ is a function to be defined. We can then obtain a linear equation for B_z from the z-component of the curl of Ampère's Law (Neukirch 1995)

$$\Delta B_z + \alpha^2 B_z - \xi(z) \left[\frac{\partial^2 B_z}{\partial x^2} + \frac{\partial^2 B_z}{\partial y^2} \right] = 0. \tag{7}$$

The coefficients of this equation do not depend on x and y. Therefore we can Fourier transform Eq. (7) in the x- and y-directions,

$$B_z(x, y, z) = \iint \tilde{B}_z(k_x, k_y, z) e^{i(k_x x + k_y y)} dk_x dk_y \tag{8}$$

and obtain a Schrödinger equation

$$\frac{d^2\tilde{B}_z}{dz^2} + [\alpha^2 - k^2 + k^2\xi(z)]\tilde{B}_z = 0 \tag{9}$$

and so we know that if $\xi(z)$ is of a recognised form we can solve for B_z explicitly. However the problem remains to solve the other components of Ampère's Law. Substituting Eq. (8) into Eq. (4) and solving for $\tilde{B}_x$ and $\tilde{B}_y$ in terms of $\tilde{B}_z$ gives

$$\tilde{B}_x = \frac{i}{k_x^2 + k_y^2}(k_x\frac{d}{dz} + k_y\alpha)\tilde{B}_z \tag{10}$$

$$\tilde{B}_y = \frac{i}{k_x^2 + k_y^2}(k_y\frac{d}{dz} - k_x\alpha)\tilde{B}_z. \tag{11}$$

This suggests that the components $B_i(x, y, z)$ are linked by a function $P(x, y, z)$ with $\tilde{B}_z = (k_x^2 + k_y^2)\tilde{P}$, which is precisely the structure of MHS equilibrium treated by Neukirch & Rastätter (1999). The force-free Green's-function solution described by Chiu & Hilton (1977) also has this structure (see Eqs. (14)-(16) of that paper). Chiu & Hilton (1977) use a well-known representation for solenoidal vector fields often used for force-free fields (see e.g. Chandrasekhar 1961; Nakagawa & Raadu 1972) which allows them to calculate the magnetic field components by solving a single scalar equation, before using an eigenfunction expansion method to derive their Green's function solution. Neukirch & Rastätter (1999) show how this special representation for the magnetic field reveals an intrinsic relationship between linear force-free fields and our special class of MHS fields. Such a link therefore opens up the possibility of reducing the problem of solving all three components of Eq. (4) for the three magnetic field components to that of solving a single scalar equation for P, as described by Neukirch & Rastätter (1999), and of using its solution to derive a Green's function solution to Eqs. (1)-(3). We will summarise the method of Neukirch & Rastätter (1999) before applying it to deriving such a solution.

The advantage of using this representation for $\mathbf{B}$ is that we can reduce the problem of calculating the complete field to that of solving one equation for the scalar quantity P. If we guarantee $\nabla \cdot \mathbf{B} = 0$ by using the following representation for $\mathbf{B}$ (cf. Nakagawa & Raadu 1972)

$$\mathbf{B} = \nabla \times (\nabla \times (P\hat{\mathbf{z}}) + T\hat{\mathbf{z}}) \tag{12}$$

then we can solve Ampère's law by letting

$$T = \alpha P, \;\; \Delta P + \alpha^2 P + gF = 0. \tag{13}$$

Now if we simplify Eq. (1) by letting

$$F = \frac{1}{g}\xi(z)B_z \tag{14}$$

with $\xi(z)$ arbitrary, Eq. (13) becomes (see Neukirch & Rastätter 1999)

$$\Delta P + \alpha^2 P - \xi(z)\left[\frac{\partial^2 P}{\partial x^2} + \frac{\partial^2 P}{\partial y^2}\right] = 0 \tag{15}$$

and we have reduced the problem to solving the scalar equation Eq. (15) for P. Now we can relate the scalar quantity P to the magnetic field via

$$\begin{aligned} B_z &= -\left(\frac{\partial^2}{\partial x^2} + \frac{\partial^2}{\partial y^2}\right)P \\ &= \frac{1}{(1-\xi(z))}\left(\frac{\partial^2 P}{\partial z^2} + \alpha^2 P\right). \end{aligned} \tag{16}$$

Note that we can recover Eq. (7) by applying $-\left(\frac{\partial^2}{\partial x^2} + \frac{\partial^2}{\partial y^2}\right)$ to Eq. (15). We will find the same solution class by solving Eq. (15) as was sought by previous authors solving Eq. (7) but without the inconvenience of having to solve the x- and y-components of Eq. (4) afterwards. When $\xi(z) < 1$, Eq. (15) is elliptic, when $\xi(z) = 1$ parabolic and when $\xi(z) > 1$ hyperbolic. The change in character of the equation as $\xi(z)$ varies through 1 is brought about by the fact that at $\xi(z) = 1$, $\nabla F \times \nabla\psi$ cancels with part of the current corresponding to P in Eq. (12).

Noting that Eq. (15) is linear and that its coefficients are independent of x and y we can Fourier transform P in the x- and y-directions,

$$P(x, y, z) = \iint \tilde{P}(k_x, k_y, z)e^{i(k_x x + k_y y)}dk_x dk_y \tag{17}$$

giving for Eq. (15)

$$\frac{d^2\tilde{P}}{dz^2} + [\alpha^2 - k^2 + k^2\xi(z)]\tilde{P} = 0. \tag{18}$$

This is a Schrödinger-type equation again, and for several forms of $\xi(z)$ we can solve Eq. (18) for $\tilde{P}$, upon which we can find P from Eq. (17) at least in the form of a Fourier-Bessel integral (see Morse & Feshbach Vol. 1, p. 766), and in the simplest cases in a closed analytical form. We can then obtain expressions for the magnetic field components by substituting P back into Eq. (12) recalling that $T = \alpha P$.

3. Green's function method

Having decided upon a convenient method for calculating the equilibria we are in a position to consider fitting boundary data. We formulate the Green's function method for this class of MHS solutions by generalising the eigenfunction expansion method employed by Chiu & Hilton (1977). For convenience we rewrite Eq. (17) as a Fourier-Bessel series in cylindrical coordinates

$$\begin{aligned} P(\rho, \phi, z) = \sum_{m=-\infty}^{\infty} e^{im\phi}\Bigg(\int_0^\infty dk \Big[&A_m(k)Q_k^{(1)}(z) \\ &+ B_m(k)Q_k^{(2)}(z)\Big] J_m(k\rho)\Bigg) \end{aligned} \tag{19}$$

where ρ, ϕ are polar coordinates in the x-y plane, $k^2 = k_x^2 + k_y^2$, ϕ is the angle between x and y (the angle between k_x and k_y has been absorbed into $A_m(k)$ and $B_m(k)$), and $Q_k^{(i)}(z)$ are the solutions of

$$\frac{d^2Q_k^{(i)}(z)}{dz^2} + [\alpha^2 - k^2 + k^2\xi(z)]Q_k^{(i)}(z) = 0. \tag{20}$$

We assume without loss of generality that $Q_k^{(1)}(0) = Q_k^{(2)}(0) = 1$ since any other finite behaviour can be absorbed into $A_m(k)$ and $B_m(k)$. Substituting P into Eq. (16) and applying Eq. (20) gives

$$\begin{aligned} B_z(\rho,\phi,z) &= \frac{1}{1-\xi(z)}\sum_{m=-\infty}^{\infty} e^{im\phi}\left(\int_0^\infty dk k^2\left[A_m(k)\right.\right. \\ &\quad \left.\left.\left(\frac{d^2}{dz^2}+\alpha^2\right)Q_k^{(1)}(z)\right]J_m(k\rho)\right) \\ &+ \frac{1}{1-\xi(z)}\sum_{m=-\infty}^{\infty} e^{im\phi}\left(\int_0^\infty dk k^2\left[B_m(k)\right.\right. \\ &\quad \left.\left.\left(\frac{d^2}{dz^2}+\alpha^2\right)Q_k^{(2)}(z)\right]J_m(k\rho)\right) \\ &= \sum_{m=-\infty}^{\infty} e^{im\phi}\left(\int_0^\infty dk k^2\left[A_m(k)Q_k^{(1)}(z)\right.\right. \\ &\quad \left.\left.+B_m(k)Q_k^{(2)}(z)\right]J_m(k\rho)\right). \end{aligned}$$

We expect only one of $Q_k^{(1)}(z)$ and $Q_k^{(2)}(z)$ to decay with height. We assume this is $Q_k^{(1)}(z)$ and that $B_m(k) = 0$. To evaluate $A_m(k)$ with respect to the boundary data we use the identities

$$\int_0^{2\pi} e^{in\phi}e^{-im\phi} = 2\pi\delta_{mn} \tag{21}$$

$$\int_0^\infty dx x J_m(\lambda x)J_m(\lambda' x) = \frac{1}{\lambda'}\delta(\lambda-\lambda') \tag{22}$$

and multiply $B_z(r,\phi,0)$ by $e^{-im\phi}J_m(k'\rho)$ then integrate it over $\int_0^\infty dr r\int_0^{2\pi} d\phi$ leading to

$$A_m(k) = \frac{1}{2\pi k}\int_0^\infty d\rho\rho\int_0^{2\pi} d\phi e^{-im\phi}J_m(k\rho)B_z(\rho,\phi,0). \tag{23}$$

Substituting $A_m(k)$ back into Eq. (19) then gives us P in a Green's function form

$$\begin{aligned} P(\rho,\phi,z) &= \frac{1}{2\pi}\int_0^\infty d\rho'\rho'\int_0^{2\pi} d\phi' \\ &\quad G_P(\rho,\phi,z,\rho',\phi',0)B_z(\rho',\phi',0) \end{aligned} \tag{24}$$

where

$$G_P(\rho,\phi,z,\rho',\phi',0) = \int_0^\infty dk\frac{1}{k}J_0(kR)Q_k^{(1)}(z) \tag{25}$$

using the identity

$$\sum_{m=-\infty}^{\infty} e^{im(\phi-\phi')}J_m(k\rho)J_m(k\rho') = J_0(kR) \tag{26}$$

with $R^2 = (x-x')^2+(y-y')^2$. The full k-spectrum from 0 to ∞ is necessary for the Green's function to have the correct behaviour at the boundary. Therefore when using the Green's function method it is not possible to reject unwanted wavenumbers for physical reasons as is done by e.g. Low (1991, 1992). As in the linear force-free case (Alissandrakis 1981; Gary 1989) the Green's function method presented here is equivalent to a Fourier integral transform method using the complete k-space.

From Eqs. (12) and (13),

$$G_x = \frac{\partial^2 G_P}{\partial x\partial z}+\alpha\frac{\partial G_P}{\partial y} = \frac{\partial R}{\partial x}\frac{\partial\bar{\Gamma}}{\partial z}+\alpha\frac{\partial R}{\partial y}\bar{\Gamma} \tag{27}$$

$$G_y = \frac{\partial^2 G_P}{\partial y\partial z}-\alpha\frac{\partial G_P}{\partial x} = \frac{\partial R}{\partial y}\frac{\partial\bar{\Gamma}}{\partial z}-\alpha\frac{\partial R}{\partial x}\bar{\Gamma} \tag{28}$$

$$G_z = -\frac{\partial^2 G_P}{\partial x^2}-\frac{\partial^2 G_P}{\partial y^2} = -\frac{\partial\bar{\Gamma}}{\partial R}-\frac{\bar{\Gamma}}{R} \tag{29}$$

where $\bar{\Gamma} = \frac{\partial G_P}{\partial R}$ (cf. Chui & Hilton (14-16)), or

$$G_R = \frac{\partial\bar{\Gamma}}{\partial z} \tag{30}$$

$$G_\theta = -\alpha\bar{\Gamma} \tag{31}$$

$$G_z = -\frac{\partial\bar{\Gamma}}{\partial R}-\frac{\bar{\Gamma}}{R}. \tag{32}$$

We remark that the structure of Eqs. (27)-(32) matches that anticipated by Eqs. (10) and (11). Writing $\bar{\Gamma}$ in the form

$$\bar{\Gamma} = \frac{\partial G_p}{\partial R} = -\int_0^\infty dk J_1(kR)Q_k^{(1)}(z), \tag{33}$$

we can calculate the Green's function components using Eqs. (30)-(32) and Bessel function identities:

$$G_R = -\int_0^\infty dk J_1(kR)\frac{d}{dz}Q_k^{(1)}(z) \tag{34}$$

$$G_\theta = \alpha\int_0^\infty dk J_1(kR)Q_k^{(1)}(z) \tag{35}$$

$$G_z = \int_0^\infty dk k J_0(kR)Q_k^{(1)}(z). \tag{36}$$

The Cartesian Green's function components can then be calculated from

$$G_x = \frac{x-x'}{R}G_R-\frac{y-y'}{R}G_\theta \tag{37}$$

$$G_y = \frac{x-x'}{R}G_\theta+\frac{y-y'}{R}G_R. \tag{38}$$

This is the structure of the Green's function solutions found by Chiu & Hilton (1977) for the force-free case, where the magnetic field is known in terms of a scalar function $\bar{\Gamma}$. We have generalised this structure to include our adopted class of MHS equilibria. Finally we can write the magnetic field in Green's function form

$$\mathbf{B}(x,y,z) = \int_{z'=0}\mathbf{G}(x-x',y-y',z)B_z(x',y',0)dx'dy' \tag{39}$$

where $\mathbf{G} = (G_x, G_y, G_z)$. This concludes the derivation of the non-force-free Green's function method for our special MHS solution class.

Except for the force-free and ξ = constant cases we only know Green's function as a Fourier-Bessel integral. Chiu & Hilton (1977) could calculate their force-free Green's function in closed form by this method only because their Fourier-Bessel

integral was to be found in the Hankel transforms literature. If $\xi(z)$ takes any other form (except $\xi(z) =$ constant) the resulting Fourier-Bessel integral cannot to the knowledge of the authors be treated analytically. In order to keep our discussion analytically explicit, we will concentrate on the force-free and $\xi =$ constant cases which will give us a closed analytical form for the Green's function, before describing a more complicated and practically applicable case as far as is analytically possible.

4. Special cases

4.1. Force-free case

The force-free case has already been calculated by Chiu & Hilton (1977) using the P-representation method of the last section. However, this case can also be treated using a more standard Green's function method as described in Morse & Feshbach (1953) Vol. 1. A derivation of the force-free Green's function using this method is given in the Appendix. The results are found to agree with those of Chiu & Hilton (1977) and we quote them here. The expression for $\bar{\Gamma}$ is

$$\bar{\Gamma} = \frac{z}{Rr}\cos(\alpha r) - \frac{1}{R}\cos(\alpha z) \tag{40}$$

giving for the Green's function components

$$G_R = \frac{R}{r^3}\cos(\alpha r) - \frac{z^2}{Rr^2}\alpha\sin(\alpha r) + \frac{\alpha}{R}\sin(\alpha z) \tag{41}$$

$$G_\theta = -\frac{\alpha z}{Rr}\cos(\alpha r) + \frac{\alpha}{R}\cos(\alpha z) \tag{42}$$

$$G_z = \frac{\alpha z}{r^2}\sin(\alpha r) + \frac{z}{r^3}\cos(\alpha r). \tag{43}$$

Note that this is not a unique solution since the general solution includes also a multiple of a complementary Green's function $\tilde{\mathbf{G}}$ whose constant of multiplication is not determined by the boundary conditions (see Chiu & Hilton 1977; Gary 1989; Lothian & Browning 1995). We follow these authors in ignoring contributions from $\tilde{\mathbf{G}}$ (see also Appendix). Recently, there have been several suggestions for how $\tilde{\mathbf{G}}$ could be determined by minimising the deviation of the force-free field on the boundary from the measured field (Amari et al. 1997; Wheatland 1999). Although we do not consider these possibilities here we remark that these approaches will in principle also work for the non-force-free fields discussed below. As a full assessment of this possibility would require a paper in its own right we leave the discussion for future work and include only $\mathbf{G}$ in the following.

4.2. Case $\xi(z) =$ constant

If $\xi(z) = \xi_0$ a constant then Eq. (15) becomes equivalent to the force-free case if $\xi_0 < 1$. To see this, let

$$\alpha_{ff} = \frac{\alpha}{\sqrt{1-\xi_0}}, \quad z_{ff} = \sqrt{1-\xi_0}z \tag{44}$$

so that

$$(1-\xi_0)\left[\frac{\partial^2 P}{\partial x^2} + \frac{\partial^2 P}{\partial y^2} + \frac{\partial^2 P}{\partial z_{ff}^2} + \alpha_{ff}^2 P\right] = 0 \tag{45}$$

This correspondence breaks down for $\xi_0 \geq 1$ and such cases must be treated in another way. We omit them here, however, since we are interested only in cases with relatively small cross-field currents. This approach is similar to the stretching procedure discussed by Lites et al. (1995) and to the transformation in spherical coordinates employed by Gary & Alexander (1999) to introduce non-force-free effects to their model. From substituting Eq. (44) into Eq. (40) the expression for $\bar{\Gamma}$ is

$$\bar{\Gamma} = \frac{\sqrt{1-\xi_0}z}{Rr}\cos\left(\frac{\alpha r}{\sqrt{1-\xi_0}}\right) - \frac{1}{R}\cos(\alpha z) \tag{46}$$

with $r^2 = x^2 + y^2 + (1-\xi_0)z^2$, giving for the Green's function components using Eqs. (30)-(32)

$$G_R = \sqrt{1-\xi_0}\frac{R}{r^3}\cos\left(\frac{\alpha r}{\sqrt{1-\xi_0}}\right) - (1-\xi_0)\frac{z^2}{Rr^2}\alpha\sin\left(\frac{\alpha r}{\sqrt{1-\xi_0}}\right) + \frac{\alpha}{R}\sin(\alpha z) \tag{47}$$

$$G_\theta = -\alpha\frac{\sqrt{1-\xi_0}z}{Rr}\cos\left(\frac{\alpha r}{\sqrt{1-\xi_0}}\right) + \frac{\alpha}{R}\cos(\alpha z) \tag{48}$$

$$G_z = \frac{\alpha z}{r^2}\sin\left(\frac{\alpha r}{\sqrt{1-\xi_0}}\right) + \frac{\sqrt{1-\xi_0}z}{r^3}\cos\left(\frac{\alpha r}{\sqrt{1-\xi_0}}\right). \tag{49}$$

Our strategy for finding analytically tractable worked examples in the present paper is to transform force-free solutions to constant-ξ solutions and generate self-consistent models of fields with three-dimensional pressure and density profiles (see Sect. 5).

4.3. Case $\xi(z) = ae^{-\kappa z}$

With this form of $\xi(z)$ the magnetic field is approximately force-free above a boundary layer of height $\frac{1}{\kappa}$ with a static interaction between the field and the plasma with magnitude increasing towards the photosphere (see Low 1991, 1992).

Referring to Eq. (18) we solve Schrödinger's equation

$$\frac{\partial^2 Q_k^{(i)}}{dz^2} + [\alpha^2 - k^2 + k^2 a e^{-\kappa z}]Q_k^{(i)} = 0. \tag{50}$$

Note from Eq. (50) that its general solution in the limit of large z becomes the force-free general solution, while in the limit of small z its general solution is asymptotically the constant-ξ general solution. The general solution of Eq. (50) is found as follows (see Morse & Feshbach 1953 Vol. 2, p. 1670):

Let $\eta = be^{-cz}$. Then Eq. (50) becomes

$$\frac{d^2 Q_k^{(i)}}{d\eta^2} + \frac{1}{\eta}\frac{dQ_k^{(i)}}{d\eta} + \left[\frac{\alpha^2 - k^2}{c^2\eta^2} + \frac{ak^2}{b^{\frac{\kappa}{c}}c^2}\eta^{\frac{\kappa}{c}-2}\right]Q_k^{(i)} = 0. \tag{51}$$

This is a Bessel equation if

$$\eta = \sqrt{\frac{4k^2 a}{\kappa^2}}e^{-\frac{1}{2}\kappa z}, \quad s^2 = \frac{4(k^2-\alpha^2)}{\kappa^2}. \tag{52}$$

Then the general solution is

$$Q_k^{(i)} = \tilde{M} J_s(\eta) + \tilde{N} J_{-s}(\eta) \tag{53}$$

where $\tilde{M}$ and $\tilde{N}$ are functions of k_x and k_y. Assuming that $\mathbf{B}$ vanishes as $z \to \infty$ implies $\tilde{N} = 0$. Now from Eq. (25) we can write

$$G_P = \int_0^\infty \tilde{M} J_s(\eta) J_0(kR) \frac{1}{k} dk \tag{54}$$

where we now choose $\tilde{M}$ to depend only on $k = \sqrt{k_x^2 + k_y^2}$. From Eq. (33),

$$\bar{\Gamma} = \frac{\partial G_p}{\partial R} = -\int_0^\infty dk J_1(kR) \tilde{M} J_s(\eta). \tag{55}$$

Now we can calculate the Green's function components using Eqs. (34)-(36):

$$\begin{aligned} G_R &= \int_0^\infty dk J_1(kR) \tilde{M} (-\sqrt{4k^2 a} e^{-\kappa z} J_{s+1}(\eta) \\ &\quad + \sqrt{4(k^2 - \alpha^2)} J_s(\eta)) \end{aligned} \tag{56}$$

$$G_\theta = \alpha \int_0^\infty dk J_1(kR) \tilde{M} J_s(\eta) \tag{57}$$

$$G_z = \int_0^\infty dk k J_0(kR) \tilde{M} J_s(\eta) \tag{58}$$

If we choose $\tilde{M}$ so that

$$\tilde{M} J_s \left(\sqrt{\frac{4k^2 a}{\kappa^2}} \right) = 1 \tag{59}$$

then we have as $z \to 0$

$$G_z \to \int_0^\infty J_0(kR) k dk = \frac{1}{R} \delta(R), \tag{60}$$

giving G_z the desired unit two-dimensional delta function behaviour on the boundary. Taking the limit as $z \to \infty$

$$\begin{aligned} \tilde{M} J_s(\eta) &\approx \frac{\left(\frac{1}{2} \sqrt{\frac{4k^2 a}{\kappa^2}} e^{-\kappa z} \right)^s}{\Gamma(s+1)} \Bigg/ \frac{\left(\frac{1}{2} \sqrt{\frac{4k^2 a}{\kappa^2}} \right)^s}{\Gamma(s+1)} \\ &= e^{-\sqrt{k^2 - \alpha^2} z} \end{aligned} \tag{61}$$

and we have recovered the eigenfunction for Eq. (20) with $\xi(z) = 0$. Our solution is asymptotically force-free at large heights.

Note that we can treat the case $\xi(z) = a e^{-\kappa z} + c$ by transforming to the case $c = 0$ as in Sect. 4.2. We anticipate that a description a coronal magnetic field by this class of Green's function solutions will be calculated using a solution with this form of ξ as it appropriately models the concentration of the interaction of the magnetic field with the plasma to near the photosphere. To keep the mathematics simple we use in our illustrative example solution a constant ξ.

5. Illustrative example: $\xi(z) =$ constant

Having derived the Green's function for the upper half space we illustrate the method with a simple example. To obtain an analytical expression for the magnetic field we generate boundary flux at $z = 0$ by putting point magnetic sources a small distance under the photosphere:

$$B_z(x, y, a) = \sum_i w_i \delta(x - x_i, y - y_i, z - a). \tag{62}$$

for some small negative a. We must have $z = a$ below the boundary in order to ensure that the magnetic field and also the plasma pressure and density are finite in the volume of interest, but otherwise a is a free parameter. We restrict our selves to point magnetic sources at points (x_i, y_i, a) in this example so that we can easily obtain closed analytical expressions for the magnetic field components. We implicitly make the assumption that the current density below the photosphere has the same form as that above the photosphere so that the magnetic sources generate just the right boundary field at $z = 0$. We emphasise that in principle we could calculate the magnetic field and plasma quantities for any given distribution of B_z on $z = 0$ and that we use this particular configuration in our example only for computational convenience.

From Eq. (39)

$$\mathbf{B}(x, y, z) = \sum_i w_i \mathbf{G}(x - x_i, y - y_i, z - a). \tag{63}$$

Denoting by $p_B(z)$ the hydrostatic background pressure, the plasma pressure and density can be found from

$$p(x, y, z) = p_B(z) - \frac{1}{2\mu_0} \xi_0 B_z(x, y, z)^2 \tag{64}$$

$$\rho(x, y, z) = -\frac{1}{g} \frac{dp_B}{dz} + \frac{1}{\mu_0 g} \mathbf{B} \cdot (\nabla(\xi_0 B_z)) \tag{65}$$

both of which have to be kept positive and non-singular in $z \geq 0$. This is clearly not possible for $a = 0$ because $\mathbf{G}$ is singular at the position of the source. Assuming the plasma to be an ideal gas it is possible to define the temperature by

$$T = \frac{\mu}{\mathrm{k_B}} \frac{p}{\rho} \tag{66}$$

where $\mu =$ mean molecular weight and $\mathrm{k_B} =$ Boltzmann constant.

The particular example we consider has two flux sources (monopoles) underneath the photospheric boundary. The magnetic field therefore has the shape of a three-dimensional magnetic flux tube with strong field inside the tube and a drop-off of the field strength with increasing distance from the tube. The example is completed by a model for the background atmosphere which is to mimic the average solar atmosphere from photoshpere through chromosphere and transition region up to the corona. To achieve this we have chosen a background temperature profile $T_B(z)$ given by

$$T_B(z) = T_0 + \Delta T \tanh \left(\frac{z - z_0}{\Delta z} \right) \tag{67}$$

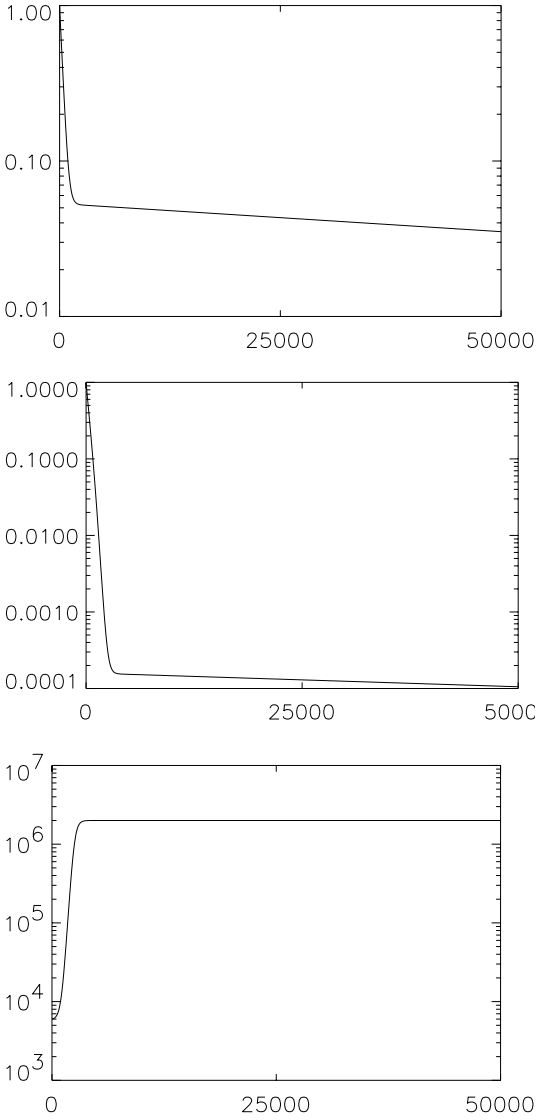

Fig. 1. Plots of the background hydrostatic equilibrium plasma parameters (vertical axes) against height (horizontal axes). Top: background pressure. Middle: background density. Bottom: background temperature. The background parameter profiles are in dependent of x and y so that any three-dimensionality in the final profiles is caused by non-force-free interaction between the plasma and the magnetic field.

where T_0 is the temperature at $z = 0$, ΔT is the difference between the temperature at $z = 0$ and the asymptotic temperature for $z \to \infty$, and z_0 and Δz are the position and width of the model transition region respectively. The hydrostatic equilibrium equation

$$\frac{dp_B}{dz} = -\rho_B g = -\frac{\mu p_B}{k_B T_B} g \tag{68}$$

is used to calculate the pressure. Finally the background density $\rho_B(z)$ is calculated from Eq. (66). Fig. 1 shows plots of the background pressure $p_B(z)$, background density $\rho_B(z)$ and background temperature $T_B(z)$ against height used in this example.

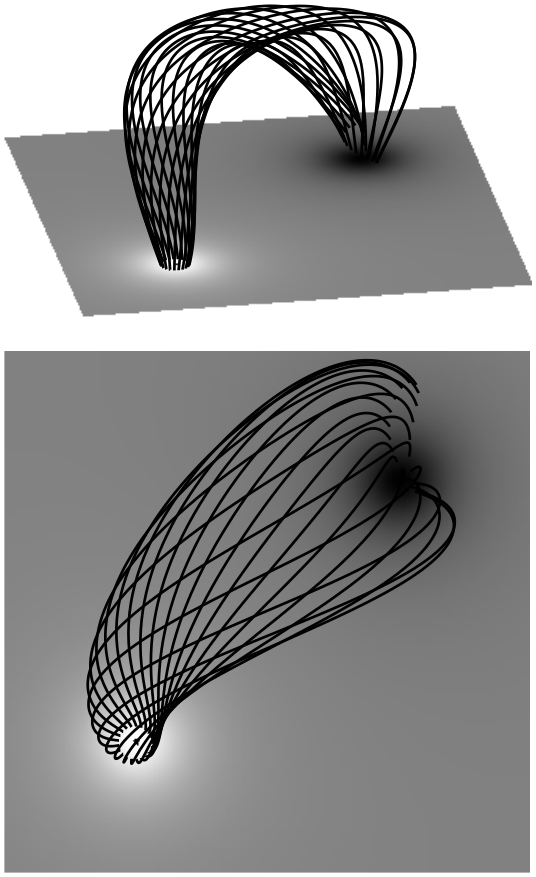

Fig. 2. Field line plot of example with $\alpha = 0.5$ and $\xi_0 = -0.1$ (top) with view from above (bottom). Shown are 20 field lines with one foot point on a circle of radius 0.3125 centred above the monopole of positive polarity. The field is generated by two submerged ($z = -1.0$) sources of equal but opposite strength.

Fig. 2 shows a set of 20 magnetic field lines having their footpoints on a circle centred above the positive polarity source. In the example shown the length scale is $L = 5000\mathrm{km}$. The square domain of the plot extends from $-5L$ to $5L$ in both x and y, and shows the vertical magnetic field strength and polarity in grey scale from maximum positive (white) to maximum negative (black). The sources are located at $z_+ = z_- = -1.0$ beneath the photosphere at the positions $(x_+, y_+) = (-2.5L, -2.5L)$ for the positive flux source and $(x_-, y_-) = (2.5L, 2.5L)$ for the negative source. In the example shown we use the values $\alpha = 0.5$ and $\xi_0 = -0.1$. The field-aligned currents cause a visible twisting of the field lines. This is in contrast to the potential field case $\alpha = \xi_0 = 0$ where the field lines are not twisted (see Fig. 3). That the effect of the cross-field currents on the magnetic field is relatively small becomes clear if one compares this example with the corresponding force-free case ($\xi_0 = 0$, see Fig. 4). Different values of $\xi_0 \neq 0$ do not alter the fieldlines significantly. The spatial variation of the plasma parameters, however, is noticeably changed by the presence of the cross-field currents. The three-dimensional structure of the pressure function can be seen in detail by comparing Figs. 5 with Fig. 6. Fig. 7 shows a pressure isosurface which in the force-free case

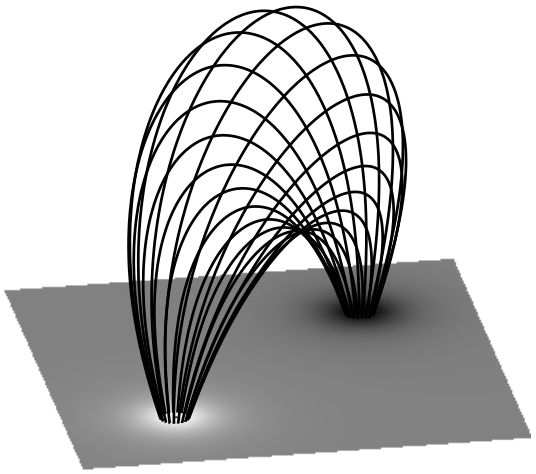

Fig. 3. Field line plot of example with $\alpha = 0.0$ and $\xi_0 = 0.0$. See caption to Fig. 2 for more details.

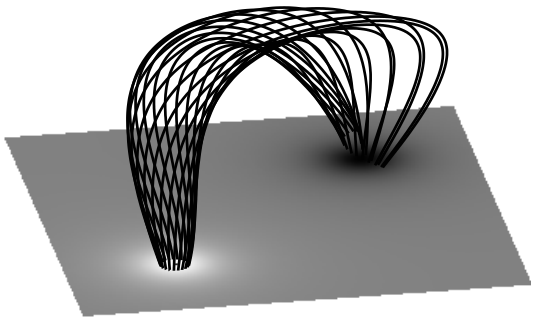

Fig. 4. Field line plot of example with $\alpha = 0.5$ and $\xi_0 = 0.0$. See caption to Fig. 2 for more details.

would be a plane parallel to the photosphere. The presence of the current especially in the regions of strong field distorts the isosurface. Two humps at the intersection of the flux tube with the surface indicate that the pressure increases inside the tube region. Referring to Eq. (64) this is to be expected because ξ_0 is negative and therefore p increases above the background level as B_z increases. The density and temperature profiles can also be seen to be significantly different from their one-dimensional backgrounds, complicated three-dimensional structures influenced by the magnetic field configuration being clearly visible in Figs. 8-12.

Figs. 13 and 14 indicate how the deviation of the pressure and density parameters from the background is related to the constants α and ξ_0. Minimum, maximum, minimum modulus and maximum modulus over the volume $(x, y, z) \in [-5.0, 5.0] \times [-5.0, 5.0] \times [0.0, 10.0]$ of $p - p_{back}$ and $\rho - \rho_{back}$ were taken in turn for discrete combinations of values of α and ξ_0. The resulting minima and maxima for the different parameter combinations are graphed against their parameter values in Figs. 13 and 14.

Many of the constant-ξ examples have some negative density in the domain. For $\xi_0 = 0$ the deviation from background hydrostatic equilibrium of all quantities is zero because this is the force-free case. For α from about -0.6 to 0.4 with ξ_0

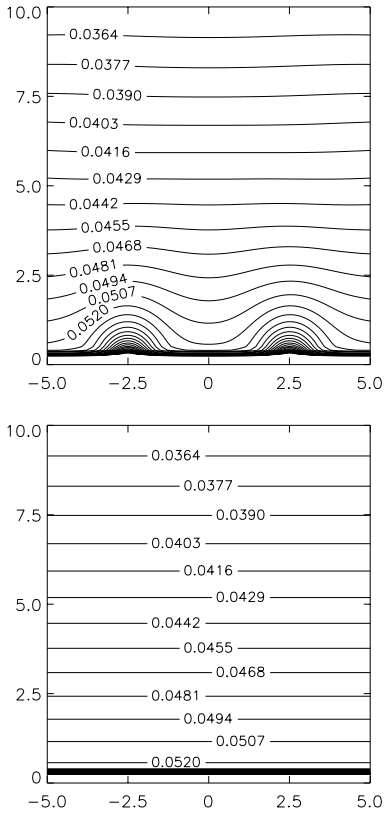

Fig. 5. Contour plots of the pressure variation in the planes $x = y$ (top) and $x = -y$ (bottom). In the plane $x = -y$ the pressure does not vary significantly from the background pressure (see Fig. 6). In the $x = y$ plane pressure deviation from background is particularly significant near the magnetic flux sources ($x = y \approx \pm 2.5$, z small) and the contours are affected to the top of the plot. Any pressure deviation from the background is an increase in this example.

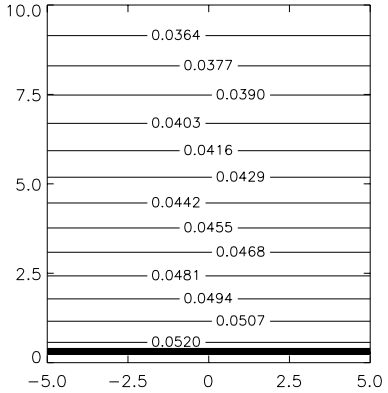

Fig. 6. Contour plot of the background pressure variation. The background pressure varies only with z hence all contours are horizontal. This is how Fig. 5 would appear in the force-free ($\xi_0 = 0$) case.

negative the pressure and density stay non-negative as for all force-free examples but for other parameter values there are problems. The pressure graphs, Fig. 13, are all symmetric about $\alpha = 0$ because of the B_z^2-dependence of Eq. (64). For all values of α and ξ_0 tested the pressure coincides with the background pressure at some point. For $\xi_0 > 0$ the pressure is less than or

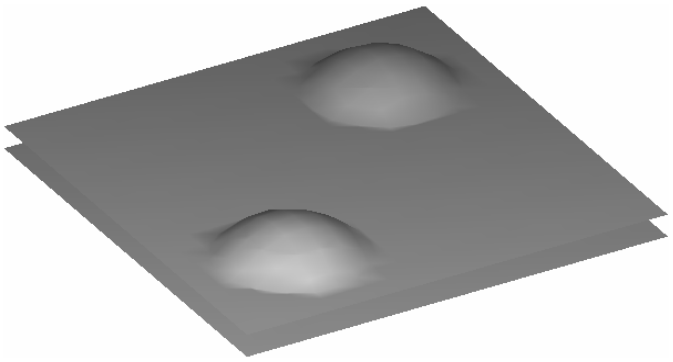

Fig. 7. Pressure isosurface $p = 0.054$. The magnetic field influences the plasma significantly where the pressure isosurface deviates from the horizontal background profile. As indicated in Fig. 5 pressure deviation from background is concentrated to the regions immediately above the two flux sources.

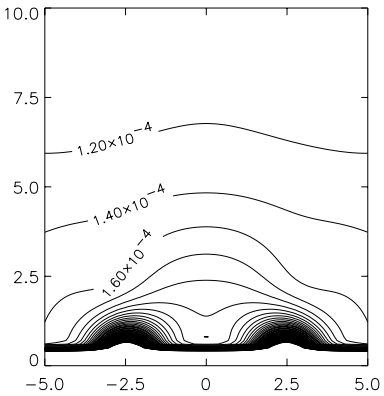

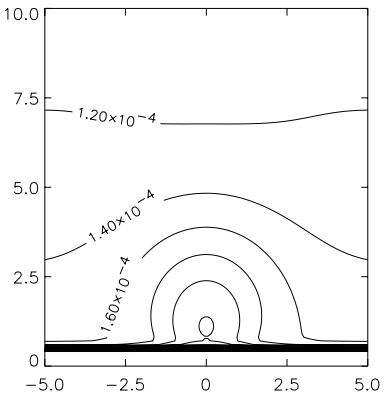

Fig. 8. Contour plots of the density variation in the planes $x = y$ (top) and $x = -y$ (bottom). Comparison with Fig. 9 shows that there is density variation from background in both planes. Density increases over background are visible in regions close to the magnetic flux sources ($x = y \approx \pm 2.5$, z small) and in a loop-like structure connecting these two regions (see Fig. 10).

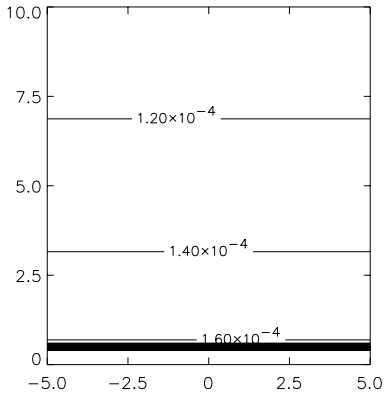

Fig. 9. Contour plot of the background density variation. The background density varies only with z hence all contours are horizontal. This is how Fig. 8 would appear in the force-free ($\xi_0 = 0$) case.

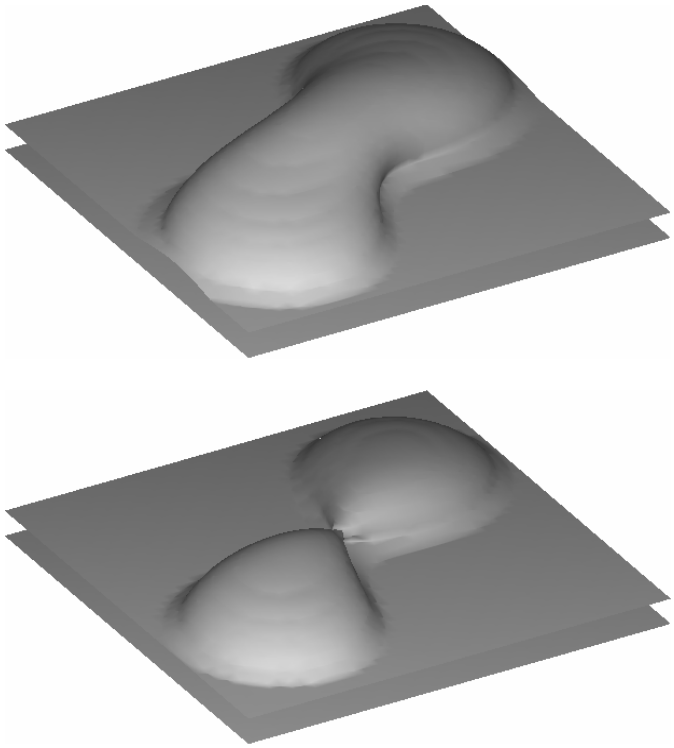

Fig. 10. Density isosurfaces $\rho = 0.0002$ (top) and $\rho = 0.000221$ (bottom). The $\rho = 0.000221$ indicates a slight density concentration above the density sources. The $\rho = 0.00020$ isosurface resembles a loop-like structure of increased density against background.

equal to the background pressure. For all parameter value combinations tested there is always some point where the pressure coincides with the background pressure and there is always a pressure drop against background somewhere. Meanwhile for $\xi_0 < 0$ the pressure is greater than or equal to the background pressure. For all parameter value combinations tested there is always some point where the pressure coincides with the background pressure and there is always a pressure increase against background somewhere.

Referring now to Fig. 14, for all values of α and ξ_0 tested the density coincides with the background pressure at some point. For $\xi_0 \neq 0$ a point where the density is less than background always exists, as does a point where the density is greater than background, indicating that mass displacement from the background density profile occurs in the volume of interest for this non-force-free case.

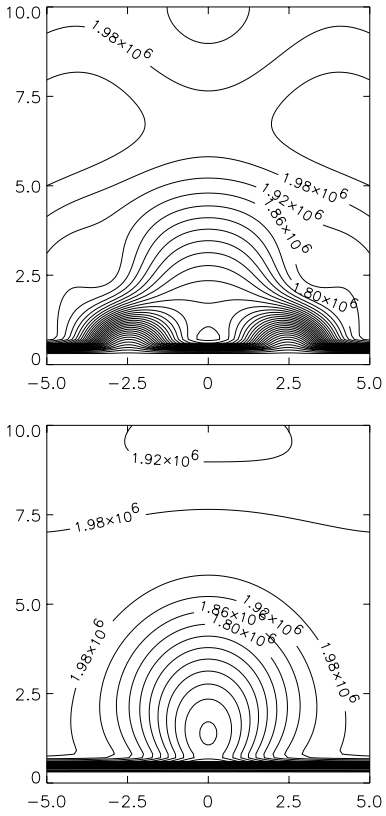

Fig. 11. Contour plots of the temperature variation in the planes $x = y$ (top) and $x = -y$ (bottom). Comparison with the background temperature profile in Fig. 1 shows that there is variation from background in both planes. There are temperature depletions from the background near the magnetic flux sources ($x = y \approx \pm 2.5$, z small) and in a loop-like structure connecting these two regions suggesting along with the density plots a structure of plasma slightly cooler and denser than the surroundings connecting the two regions above the magnetic flux sources (see Fig. 12. The background temperature is constant except for small values of z (see Fig. 1), where it varies only with z hence all contours would be horizontal.

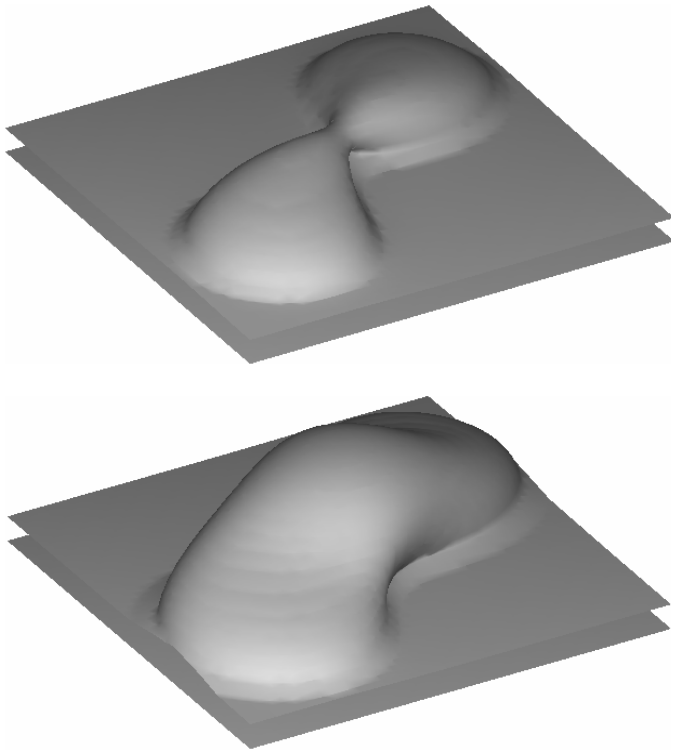

Fig. 12. Temperature isosurfaces $T = 1.38 \times 10^6$ (top) and $T = 1.60 \times 10^6$ bottom. The pictures show a relatively cool loop-like structure between regions of low temperature, which are concentrated above the magnetic flux sources.

6. Discussion

We have derived the Green's function method for a particular class of MHS equilibria for which the current density is a combination of a linear force-free part and a part with non-force-free components. The method was developed by extending an existing linear force-free field Green's function method and by exploiting a recently-discovered relationship between linear force-free fields and the class of MHS equilibria. Existing Green's function methods for linear force-free fields allow only an indirect comparison between extrapolated coronal field-lines and observed parameter profiles. This MHS Green's function method therefore provides the first opportunity for a direct comparison between a coronal magnetic field model and observation. An artificial intensity map may be constructed from the model for direct comparison with an observed intensity map. We have also presented in an Appendix a new derivation of the linear force-free Green's function based on textbook theory for the Helmholtz equation. This places the nonstandard eigenfunction expansion method used elsewhere in agreement with standard textbook theory.

We have prepared the solutions anticipating fitting the vertical magnetic field component on the photosphere. In fact, Semel (1988) has presented a method of fitting line-of-sight data to a linear force-free Green's function solution but his idea is not easily applied to our scheme because of the strictly vertical influence of gravity. It remains to be seen how much of a practical limitation this will be when we try to fit our solutions to observational data.

Appendix A: Textbook method for force-free Green's function

We include this approach here to show that standard textbook Green's function method is equivalent to the non-standard approach based on the P-representation where both are applicable. The z-component of curl of Ampère's law is Helmholtz's equation

$$\Delta B_z + \alpha^2 B_z = 0 \tag{A.1}$$

We follow the established Green's function method for Helmholtz's equation as described in Morse & Feshbach (1953), Vol. 1. For our force-free example, the required Green's function solves

$$\Delta G_z(\mathbf{r}, \mathbf{r}') + \alpha^2 G_z(\mathbf{r}, \mathbf{r}') = -\delta(\mathbf{r} - \mathbf{r}'). \tag{A.2}$$

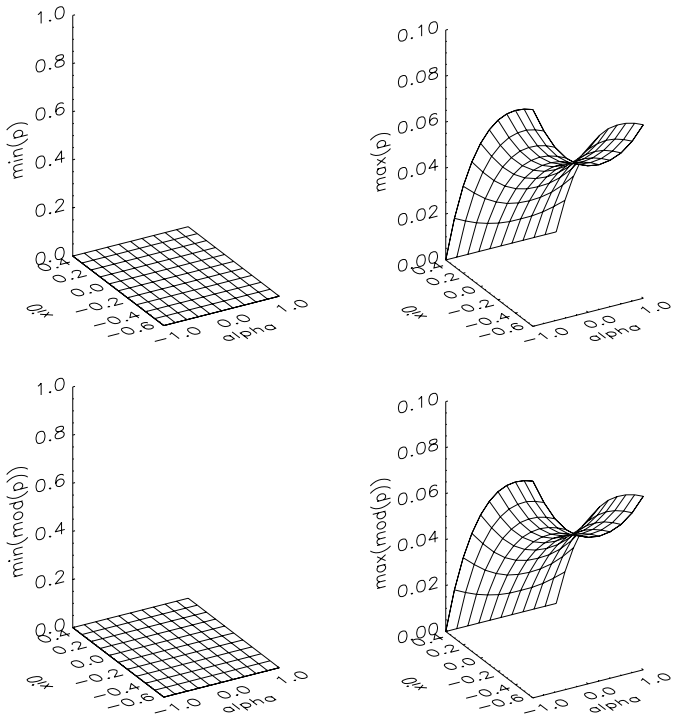

Fig. 13. Top left: $\min(p - p_{back})$ for a range of values of α and ξ_0. Top right: $\max(p - p_{back})$. Bottom left: $\min|p - p_{back}|$. Bottom right: $\max|p - p_{back}|$.

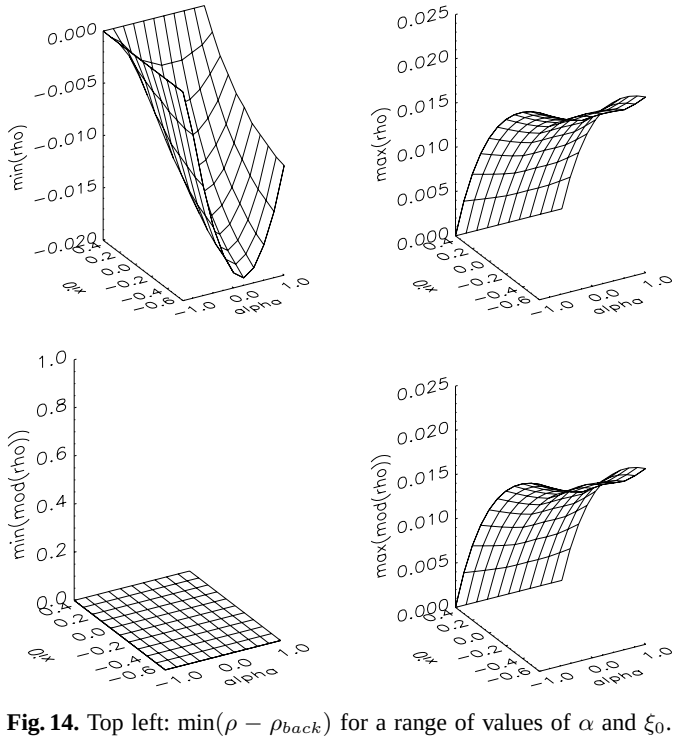

Fig. 14. Top left: $\min(\rho - \rho_{back})$ for a range of values of α and ξ_0. Top right: $\max(\rho - \rho_{back})$. Bottom left: $\min|\rho - \rho_{back}|$. Bottom right: $\max|\rho - \rho_{back}|$.

Solving by Fourier transforms we obtain

$$G_z(\mathbf{r}, \mathbf{r}') = g_z(r) = \frac{\cos(\alpha r)}{r}. \tag{A.3}$$

Solving for the homogeneous solution of Eq. (A.2) assuming that $G_z(\mathbf{r}, \mathbf{r}') = g_z(r)$ we have

$$g_z = \frac{a' \cos \alpha r}{r} + \frac{b' \sin \alpha r}{r} \tag{A.4}$$

but from Eq. (A.3) only $\frac{\cos(\alpha r)}{r}$ gives the desired delta-function behaviour at $r = |\mathbf{r} - \mathbf{r}'| \to 0$. The second term of Eq. (A.4) corresponds to the complementary Green's function described by Chiu & Hilton (1977) and has no contribution to the magnetic field at $z = 0$. We therefore do not have sufficient observational data to determine b' uniquely, e.g. horizontal magnetic field components on the boundary, and so we follow Chiu & Hilton (1977) and concentrate on the first term of Eq. (A.4) with $a' = 1$. Taking $G_z(\mathbf{r}, \mathbf{r}') = \frac{\cos(\alpha r)}{r}$ we get

$$\begin{aligned} B_z(x, y, z) &= -\int_{z=0} B_z(\mathbf{r}') \nabla' G_z(\mathbf{r}, \mathbf{r}') \cdot d\mathbf{n} \\ &= \int_{z=0} \frac{\partial G_z}{\partial z}(x, y, z, x', y', 0) B_z(x', y', 0) dx' dy' \end{aligned}$$

where

$$\frac{\partial G_z}{\partial z} = \left(\frac{\alpha}{r} \sin(\alpha r) + \frac{1}{r^2} \cos(\alpha r) \right) \frac{z}{r}. \tag{A.5}$$

This is of the same form as Eq. (39) but with $(\mathbf{n} \cdot \nabla)\mathbf{G}$ playing the role of $\mathbf{G}$ (Morse & Feshbach (1953), Vol. 1, p. 806).

It remains to calculate B_x and B_y, and here it is most convenient to fall back on the P-representation of the field. Recalling the structure of the Green's function Eqs. (30)-(32), we need

$$\frac{\partial}{\partial R}(R\bar{\Gamma}) = -R \frac{\partial G_z}{\partial z} \tag{A.6}$$

giving for $\bar{\Gamma}$ on applying Eq. (15)

$$\bar{\Gamma} = \frac{z}{Rr} \cos(\alpha r) - \frac{1}{R} \cos(\alpha z). \tag{A.7}$$

We have recovered Chiu & Hilton's solution for $\mathbf{B}$, complete with its "P"-structure without assuming it at the beginning.

Acknowledgements. We thank the referee, Tahar Amari, for useful and constructive comments. We thank PPARC for financial support by a studentship (GP) and an Advanced Fellowship (TN).

References

Alissandrakis C.E., 1981, A&A 100, 197
Altschuler M.D., Newkirk G., 1969, Solar Phys. 9, 131
Altschuler M.D., Trotter D.E., Newkirk G., Howard R., 1974, Solar Phys. 39, 3
Altschuler M.D., Levine R.H., Stix M., Harvey J., 1977, Solar Phys. 51, 345
Aly J.J., 1989, Solar Phys. 120, 19
Amari T., Démoulin P., 1992, In: Proceedings of Workshop: Méthodes de détermination des champs magnétiques solaires et stellaires. Observatoire de Paris, p. 187
Amari T., Aly J.J., Luciani J.F., Boulmezaoud T.Z., Mikic Z., 1997, Solar Phys. 174, 129
Amari T., Boulmezaoud T.Z., Mikic Z., 1999, A&A 350, 1051

Aulanier G., Démoulin P., Schmeider B., Fang C., Tang Y.H., 1998, Solar Phys. 183, 369
Aulanier G., Démoulin P., van Driel-Gesztelyi L., Mein P., DeForest C., 1999, A&A 342, 864
Bagenal F., Gibson S., 1991, J. Geophys. Res. 96, 17663
Barbosa D.D., 1977, Solar Phys. 56, 55
Bogdan T.J., Low B.C., 1986, ApJ 306, 271
Chandrasekhar S., 1961, Hydrodynamic and Hydromagnetic Stability. Oxford University Press
Chiu Y.T., Hilton H.H., 1977, ApJ 212, 873
Démoulin P., Hénoux J.C., Mandrini C.H., Priest E.R., 1997, Solar Phys. 174, 73
Gary G.A., 1989, ApJS 69, 323
Gary G.A., 1997, Solar Phys. 174, 241
Gary G.A., Alexander D., 1999, Solar Phys. 186, 123
Gibson S., Bagenal F., 1995, J. Geophys. Res. 100, 19865
Lee J., White S.M., Kundu M.R., Mikic Z., McClymont A.N., 1999, ApJ 510, 413
Lites B.W., Low B.C., Martinez Pillet V., et al., 1995, ApJ 446, 877
Lothian R.M., Browning P.K., 1995, Solar Phys. 161, 289
Low B.C., 1985, ApJ 293, 31
Low B.C., 1991, ApJ 370, 427
Low B.C., 1992, ApJ 399, 300
Low B.C., 1993a, ApJ 408, 689
Low B.C., 1993b, ApJ 408, 693
McClymont A.N., Mikic Z., 1994, ApJ 422, 899
McClymont A.N., Jiao L., Mikic Z., 1997, Solar Phys. 174,, 191
Morse P.M., Feshbach H., 1953, Methods of Theoretical Physics (2 Vols.). McGraw-Hill, New York
Nakagawa Y., Raadu M.A., 1972, Solar Phys. 25, 127
Neukirch T., 1995, A&A 301, 628
Neukirch T., 1997a, A&A 325, 847
Neukirch T., 1997b, Phys. Chem. Earth 22, 405
Neukirch T., Rastätter L., 1999, A&A 348, 1000
Roumeliotis G., 1996 ApJ 473, 1095
Sakurai T., 1981, Solar Phys. 69, 343
Sakurai T., 1982, Solar Phys. 76, 301
Schatten K.H., Wilcox J.M., Ness N.F., 1969, Solar Phys. 6, 442
Schmidt H.V., 1964, In: Ness W.N. (ed.) ASS-NASA Symposium on the Physics of Solar Flares. NASA SP-50, p. 107
Semel M., 1967, Ann. Astrophys. 30, 513
Semel M., 1988, A&A 198, 293
Wheatland M.S., 1999, ApJ 518, 948
Wu S.T., Chang H.M., Hagyard M.J., 1985, In: Hagyard M.J. (ed.) Measurements of Solar magnetic Fields. NASA CP-2374, p. 17
Zhao X., Hoeksema J.T., 1993, Solar Phys. 143, 41
Zhao X., Hoeksema J.T., 1994, Solar Phys. 151, 91